An Efficient Full-Wave Method for Analysis of Dielectric Resonators Possessing Separable Geometries Immersed in Inhomogeneous Environments

Shu-Li Lin and George W. Hanson, *Senior Member, IEEE*

Abstract—In this paper, dielectric resonators possessing separable-coordinate geometries immersed in planarly-inhomogeneous media are analyzed using a volume electric-field integral-equation (IE)/Galerkin's technique. A three-dimensional complete entire-domain basis function set is utilized in numerically solving the IE. It is shown that a few terms of one physically significant subset of basis functions are usually sufficient for the accurate determination of complex resonant frequencies of cylindrical and rectangular resonators immersed in homogeneous and planarly inhomogeneous environments. The results using a few basis functions show good agreement with the previous literature, and new results are presented for some rectangular resonator geometries.

Index Terms—Dielectric antennas, dielectric resonators, integral equations, nonhomogeneous media.

I. INTRODUCTION

DIELECTRIC resonators (DR's) are important elements of microwave integrated circuits (MIC's), and are also used as millimeter-wave resonators and DR antennas. DR's are useful due to their small size, mechanical simplicity, relatively large bandwidth, and their absence of conduction loss [1]. They are also easily coupled to a wide variety of transmission lines and waveguides. There are two major differences in the use of DR's for resonator and antenna applications: their background structures and typical permittivity values. For resonator applications, often a shielded structure is utilized, but for antenna applications the resonator must be placed in an open environment. In addition, for antenna applications the permittivity is often fairly low to provide sufficient impedance bandwidth, while for resonator applications the permittivity is high so that the physical size of the resonator is small. In the following, the term "resonator" is used to denote both resonator and antenna applications.

The analysis method proposed in this paper is applicable to any resonator possessing a separable coordinate geometry, but the most common shapes are a sphere, finite cylinder, or rectangular parallelepiped. Among those three, the cylindrical resonator is probably the most popular, although the rectangular one is sometimes considered easier to fabricate, and it can be constructed to avoid mode degeneracies.

When DR's are utilized in microwave or millimeter-wave applications, it is important to determine their resonant frequencies and quality factors (Q-factors). In the previous literature, there are theoretical and experimental investigations of resonant frequencies and Q-factors of isolated DR's [2]–[6]. Theoretically exact methods exist to obtain characteristics of spherical DR's in homogeneous environments [7]. Cylindrical DR's may be analyzed by efficient body of revolution integral-equation (IE) methods, but there have been few rigorous methods presented for the study of rectangular resonators other than finite elements or finite-difference techniques [8], [9], although several papers have presented measurement results [10].

In this paper, a volume electric-field integral equation (EFIE) formulation in conjunction with an entire-domain Galerkin's method-of-moments (MoM) solution is proposed to study the resonant frequencies and Q-factors of both cylindrical and rectangular DR's and coupled resonators in multilayered media. A three-dimensional (3-D) complete entire-domain basis function set is utilized in numerically solving the integral equation (IE). The basis set contains as subsets the perfect magnetic conductor (PMC) and perfect electric conductor (PEC) cavity modes, and other terms that are also observed to have physical meaning. It is shown that a few terms of the PMC modes are usually sufficient for the accurate determination of complex resonant frequencies for a very wide range of permittivity values due to the incorporation of these modes into the theoretically exact EFIE. The use of PMC models has been considered previously for DR's immersed in homogeneous environments [11], and it is well known that such approximate techniques yield fairly inaccurate results. The method presented here yields accurate results for resonators immersed in either homogeneous or inhomogeneous background environments principally due to the effect of *processing* the modes as basis and testing functions in the exact IE, which is shown to result in a stationary implicit equation for the complex resonance frequencies. Results using a few basis functions show good agreement with the previous literature, and new results are presented for some rectangular resonator geometries. Since typically only a few PMC basis functions are needed in the expansion of the unknown resonant field, the method is found to be very computationally efficient. This is especially true for nonbody-of-revolution geometries, i.e., the parallelepiped, where, for instance, a surface formulation would lead to a greater number of unknowns. The drawback of this
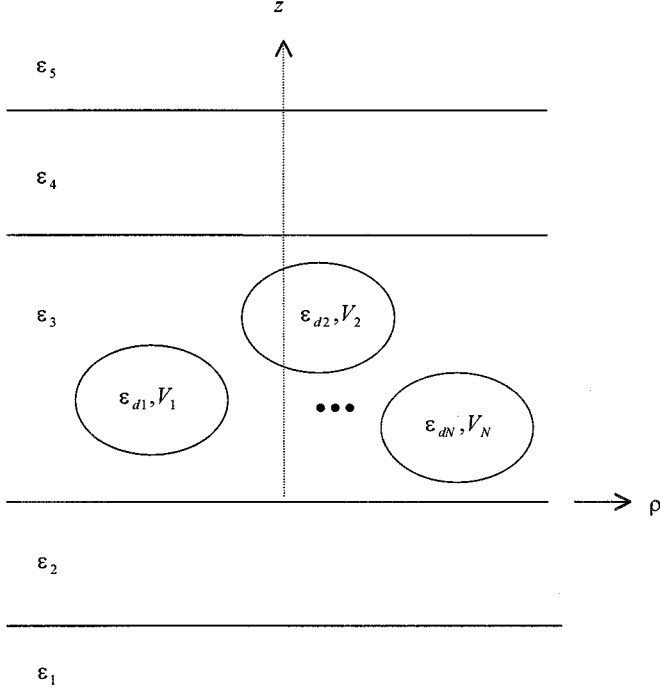
Fig. 1. Geometry of N dielectric objects immersed in a five-layer inhomogeneous medium.

method is that it is only applicable to separable-coordinate geometries, and only for frequencies near the resonance frequencies of the object. However, virtually all DR's fit into the above category and, thus, this method is found to be useful in the majority of practical cases.

II. FORMULATION

Consider N dielectric objects immersed in a planarly inhomogeneous environment, as depicted in Fig. 1. The total electric field at points in any region can be represented as $\vec{E} = \vec{E}^i + \vec{E}^s$ where $\vec{E}^i$ is an incident field and $\vec{E}^s$ is the field scattered by the objects. By the equivalent source theorem, the scattered field $\vec{E}^s$ is maintained by the equivalent induced polarization currents inside of the N dielectric objects, leading to ($e^{j\omega t}$ assumed and suppressed)

$$\vec{E}(\vec{r}) = \vec{E}^i(\vec{r}) + \sum_{i=1}^{N} \int_{V_i} \overleftrightarrow{G}^e(\vec{r}, \vec{r}') \cdot \frac{\vec{P}_i^{eq}(\vec{r}')}{j\omega\varepsilon_3} \, dV' \quad (1)$$

where $\overleftrightarrow{G}^e$ is an electric dyadic Green's function accounting for the inhomogeneous environment and relating currents located by $\vec{r}'$ in region 3 to fields located by $\vec{r}$ in any region, and $\vec{P}_i^{eq}$ is equivalent polarization current induced inside of the i'th dielectric object, which can be represented as

$$\vec{P}_i^{eq}(\vec{r}) = j\omega\left[\varepsilon_{di}(\vec{r}) - \varepsilon_3\right]\vec{E}(\vec{r}), \qquad \vec{r} \in V_i; \quad i = 1, \cdots, N. \quad (2)$$

Therefore, (1) may be written as

$$\vec{E}(\vec{r}) - \sum_{i=1}^{N} \int_{V_i} \overleftrightarrow{G}^e(\vec{r}, \vec{r}') \cdot \frac{[\varepsilon_{di} - \varepsilon_3]}{\varepsilon_3} \vec{E}(\vec{r}') \, dV' = \vec{E}^i(\vec{r}). \quad (3)$$

While (3) is valid for any $\vec{r}$, the restriction $\vec{r} \in V = \sum_{i=1}^{N} V_i$ leads to the standard formulation for determining the volume polarization current (2). Subsequent to determining $\vec{P}_i^{eq}$, the scattering field in any region is easily determined.

When studying natural resonance problems, the incident field vanishes, leading to the homogeneous EFIE

$$\vec{E}(\vec{r}) - \sum_{i=1}^{N} \int_{V_i} \overleftrightarrow{G}^e(\vec{r}, \vec{r}') \cdot \frac{[\varepsilon_{di} - \varepsilon_3]}{\varepsilon_3} \vec{E}(\vec{r}') \, dV' = 0. \quad (4)$$

Assuming the N dielectric objects are homogeneous, the EFIE can be rewritten as

$$\vec{E}(\vec{r}) - \sum_{i=1}^{N} \frac{[\varepsilon_{di} - \varepsilon_3]}{\varepsilon_3} \int_{V_i} \overleftrightarrow{G}^e(\vec{r}, \vec{r}') \cdot \vec{E}(\vec{r}') \, dV' = 0. \quad (5)$$

The unknown electric field can be expanded as

$$\vec{E}(\vec{r}) = \sum_{(m, n, p)} a^{(m, n, p)} \vec{K}_{(m, n, p)}(\vec{r}) \quad (6)$$

where $\vec{K}_{(m, n, p)}(\vec{r})$ is an appropriate set of expansion functions, which will be detailed in Section III. By testing with the same set of functions, which is Galerkin's procedure, we arrive at a block matrix system

$$\left[Z_{lk}(f)\right][A_k] = 0. \quad (7)$$

We use the Galerkin's method here since this leads to enhanced convergence of the spectral integrals associated with the Green's function, compared to, say, point matching. In (7), the lk element of the impedance matrix represents the reaction [12] between the lth (m, n, p) mode testing function on the kth (m, n, p) mode expansion function. After forming the matrix system, we search for nonstandard eigenvalues f in the complex frequency plane from

$$\det\left[Z(f)\right] = 0 \quad (8)$$

with complex frequency $f = f_{\text{real}} + jf_{\text{imag}}$. The Q-factor is defined as $f_{\text{real}}/2f_{\text{imag}}$. Assuming that the complex resonant frequency is a simple root of the determinant function (8), the vector of unknown coefficients can be determined to within an arbitrary constant by fixing one coefficient in $Z(f)A = 0$ and solving the resulting set of equations for the remaining unknown.

Although we do not have the space to discuss many details of the computation here, the Green's functions are thoroughly discussed in [13] for polar coordinates and in [14] for rectangular coordinates. The resulting rectangular coordinate Sommerfeld integrals are computed in the polar form $\int_0^{\pi/2} d\theta \int_0^\infty F(\theta, \lambda)\lambda \, d\lambda$, which results in $F(\theta, \lambda)$ being fairly smooth as a function of λ for all values of θ, and good convergence properties of the semiinfinite integral for all values of θ, except at the end points $(\theta = 0, \pi/2)$. Furthermore, the semiinfinite integral is computed over a path that avoids the singularities of the integral (see, e.g., [15], [16]). The integrals are computed using a Romberg procedure modified from [17], where the tail of the semiinfinite integral is computed using an adaptive routine, which truncates the integration when convergence is satisfied.

III. BASIS FUNCTION SET

To understand the basis set utilized here, first consider the one-dimensional (1-D) problem of a transmission-line resonator extending over $[-(a/2), a/2]$ with short- or open-circuit boundary conditions. Since the set $S_I^x = \{1, \cos((2m\pi/a)x), \sin((2m\pi/a)x)\}$ with $m = 0, 1, 2, \cdots$, is complete on $L^2[-(a/2), a/2]$, any physically realistic voltage $v(x) \in L^2[-(a/2), a/2]$ can be exactly represented (in the L^2-norm sense) as a sum of terms in S_I^x. 1-D physical resonances for the short-circuited resonator take on the form of integer multiples of half-wave sinusoidal variation, corresponding to $m = 1/2, 3/2, 5/2, \cdots$, for the term $\cos((2m\pi/a)x)$, and $m = 1, 2, 3, \cdots$, for the term $\sin((2m\pi/a)x)$, with the important fundamental resonance given by $\cos((2m\pi/a)x)$, $m = 1/2$. For an open-circuit resonator, the resonances are given by $m = 1, 2, 3, \cdots$, for the $\cos((2m\pi/a)x)$ term and $m = 1/2, 3/2, 5/2, \cdots$, for the $\sin((2m\pi/a)x)$ term. Therefore the complete set S_I^x contains resonance-like behavior in the sine (cosine) terms, but not the cosine (sine) terms for the short (open)-circuited case, although the missing resonances in either case can be synthesized by the complete set S_I^x through a sum of terms as in a Fourier series.

To more efficiently represent the missing voltage resonances in S_I^x, consider the set $S_{NI}^x = \{\cos((2m\pi/a)x), \sin((2m\pi/a)x)\}$ with $m = 1/2, 3/2, 5/2, \cdots$. The terms $\cos((2m\pi/a)x)$ in S_{NI}^x will represent physical resonances for the short-circuited case, whereas the $\sin((2m\pi/a)x)$ terms represent physical resonances for the open-circuited case. The set $S^x = S_I^x \cup S_{NI}^x$, the terms of which represent all possible physical resonances for both types of boundary conditions, is an over-complete set containing the complete set S_I^x and the additional terms in S_{NI}^x. The utility of using the set S^x is that one can accurately model any (ideal) resonance phenomena with one term of the set for either boundary condition, rather than possibly needing to synthesize the proper behavior with a sum of terms of S_I^x. Therefore, when interested in resonance phenomena, we can expand any $v(x) \in L^2[-(a/2), a/2]$ function in the over-complete set S^x, where generally only one term would be needed to model any possible resonance assuming that the proper expansion coefficient can be found. The set S^x is not linearly independent (orthogonal) on $[-(a/2), a/2]$, yet subsets S_I^x and S_{NI}^x are orthogonal among themselves.

An alternative view of the proceeding is to consider the interval $[-a, a]$, on which the set S^x is now complete and orthogonal, and to consider the voltage to have compact support on $[-(a/2), a/2]$ (i.e., the physical resonator extends over that range). In this latter conceptualization, the proper expansion coefficients are easily seen to be the Fourier coefficients. Either viewpoint is applicable to the method presented here.

In the previous transmission-line resonator example one is usually interested in the short-circuited (electrical wall) or open-circuited (magnetic wall) case, but not both conditions simultaneously. For DR problems, field continuity rather than the vanishing of tangential electric field (electric wall) or tangential magnetic field (magnetic wall) is enforced. For a 1-D DR, if the permittivity ratio $\varepsilon_d/\varepsilon_3 \gg 1$ occurs, the resonance modes will behave approximately as open-circuited resonances, while
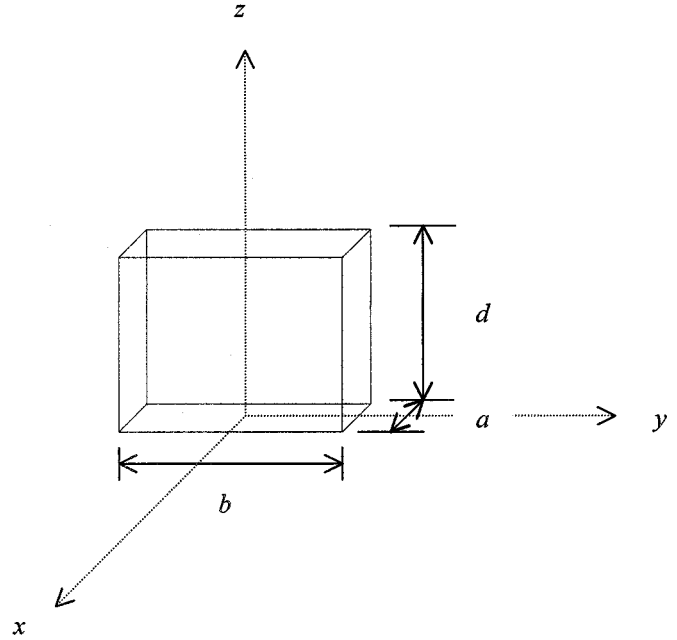

Fig. 2. Geometry of a rectangular cavity.

for $\varepsilon_d/\varepsilon_3 \ll 1$, the resonant modes will behave approximately as short-circuited resonances. For arbitrary $\varepsilon_d/\varepsilon_3$, both types of resonance terms may occur and, thus, it is useful to expand the unknown in terms of the set S^x.

Consider now a 3-D rectangular volume, as depicted in Fig. 2, over which the EFIE (5) will be enforced. Even though the electric field extends over all space, and for natural-mode fields (which are associated with complex resonant frequencies in the upper half temporal Fourier-transform plane) become unbounded (in the frequency domain) as $r \to \infty$, the integral operator acts on a bounded domain within which the field is bounded and continuous. We will consider the domain of the integral operator in (5) to be the space $L^2(V)$; the space of square-integrable vector functions $\vec{E}: V \to C^3$. Since the operator in (5) is indefinite, convergence of a numerical solution for the unknown electric field cannot perhaps be proven in a rigorous sense [18]. It may though be desirable to expand the unknown electric field in a complete set in $L^2(V)$; it is at least necessary for the expansion set to span some subset of the domain containing the unknown quantity. Since this cannot be determined *a priori*, it is useful to consider the entire space $L^2(V)$. If $V = \{x, y, z | x \in [-(a/2), a/2], y \in [-(b/2), b/2], z \in [0, d]\}$, then the set $S_I = \{S_I^x, S_I^y, S_I^z\} = \{1, \cos((2m\pi/a)x), \sin((2m\pi/a)x), \cos((2n\pi/b)y), \sin((2n\pi/b)), \cos((2p\pi/d)z), \sin((2p\pi/d)z)\}$, $m, n, p = 0, 1, 2, \cdots$ is complete in $L^2(V)$ and forms an appropriate basis set for (5). As in the 1-D example, we consider the over-complete set S consisting of terms with the same functional dependence as those in S_I, but with $m, n, p = 0, 1/2, 1, 3/2, 2, \cdots$ as the expansion for the unknown field, presented as (A1) for the geometry depicted in Fig. 2. The individual sine and cosine terms in (A1) are written in shifted form, but are mathematically identical to terms of S described above. The shifted representation is used here to facilitate identification of PMC and PEC terms in the complete expansion. Note that the

product form (A1) can represent any of the singlet, doublet, or triplet terms arising from the possible combination of terms in S. Alternatively, as with the 1-D example, one can consider a larger domain over which S is complete and assume the unknown resonator fields in (5) have compact support in V.

Although the question of convergence of the MoM solution cannot be properly addressed, the MoM formulation for nonhomogeneous problems (e.g., scattering) involving complex-symmetric operators has been shown to be variational in nature for secondary calculations [19]. It is also observed from [20] that since the integral operator is complex symmetric, (8) is a stationary expression for the complex resonant frequencies such that second-order accuracy in the calculation of the resonant frequency is obtained by an approximate expansion of the unknown field exhibiting first-order error. The stationary nature of (8) was observed numerically, which is exemplified by the following example. Consider the PMC cavity solution $\vec{E}^a$, $\vec{H}^a$, which can be obtained by standard methods for a closed cavity. Substituting into Maxwell's equations leads to the resonance condition $(m\pi/a)^2 + (n\pi/b)^2 + (p\pi/d)^2 - (2\pi f_r)^2 \mu_0 \varepsilon_d = 0$ for the real resonant frequency f_r. This value is 3.932 (GHz) for the TE_{110}^z mode with $\varepsilon_d = 37.84\varepsilon_0$, $a = b = 8.77$ (mm), and $d = 3.51$ (mm), -30.4% in error compared to the value 5.6493 (GHz) obtained by solution to the IE here using the full 3-D expansion (A1), and -30.82% in error compared to the value listed in [10]. Now consider "processing" the approximate PMC solution $\vec{E}^a$ through the IE, the solution of which also satisfies Maxwell's equations. The result is a determinal equation (8), which by a numerical root search yields $f_r = 5.685$ (GHz), 0.63% in error compared with the solution of the IE using (A1), and 0.018% in error compared to the result in [10]. Thus, for the geometry considered here, (8) exhibits an error-reducing nature. It is this feature that makes the IE formulation presented here efficient since usually just the PMC terms are necessary for good accuracy, even when the ratio of permittivities $\varepsilon_d/\varepsilon_3$ is not large.

To further examine the terms in the expansion set (A1), it is seen that each unknown electric-field component has eight terms. If we inspect (A1) carefully, it is easy to find that there is one term corresponding to a PMC mode (the sixth term in (A1) for K^x and the seventh term in (A1) for K^y), one term corresponding to a PEC mode [the third term in for K^x and the second term in (A1) for K^y(A1)], and six other terms in each eight-term summation corresponding to each electric-field component. The six other terms may be interpreted as modes that have mixed PMC and PEC conditions, with the constraint that opposite walls have identical boundary conditions, as detailed in the Appendix (see Table A1). This fact should not be surprising when one notes that in a 1-D Fourier series proper functional behavior is synthesized by a sum of open-circuited (PMC) and short-circuited (PEC) terms. Thus, the PMC modes, while motivated by the physics of the problem, actually are part (one term in eight for each triplet m, n, p) of a proper mathematical representation for the problem of 3-D resonance with possible variation in all three orthogonal directions. Therefore, the role of the PMC terms for the solution of (5) is well motivated both physically and mathematically. A similar discussion can be made for the cylindrical geometry, but will be omitted here. Conversely, for $\varepsilon_d/\varepsilon_3 \ll 1$, only the PEC terms would be

TABLE I
CONVERGENCE TEST OF A CYLINDRICAL
DR IN FREE SPACE, $\varepsilon_d = 38\varepsilon_0$ (mm), $R = 5.25$ (mm), AND $D = 4.6$ (mm)

N	(n, m, p)	f_{real} (GHz)	f_{imag} (GHz)
1	(0, 1, 0)	4.8891	0.06386
2	(0, 1, 2)	4.8677	0.06164
3	(0, 2, 0)	4.8637	0.06012
4	(0, 2, 2)	4.8634	0.06007
5	(0, 3, 0)	4.8627	0.05984
6	(0, 3, 2)	4.8627	0.05983
7	(0, 4, 0)	4.8625	0.05977
8	(0, 4, 2)	4.8625	0.05977
9	(0, 5, 0)	4.8624	0.05974
10	(0, 5, 2)	4.8624	0.05974

TABLE II
RESONANCE FREQUENCY AND Q-FACTOR USING PMC MODES IN THE IE
FORMULATION COMPARED TO OTHER RESULTS FOR A CYLINDRICAL DR IN
FREE SPACE WITH $\varepsilon_d = 38\varepsilon_0$, $R = 5.25$ (mm), AND $D = 4.6$ (mm)

	Frequency (GHz)	Q-factor
Surface IE & MoM [2]	4.829	45.8
Null-Field Method [5]	4.8604	40.819
FDTD Method [3]	4.862	47
FDTD Method [4]	4.848	41
Measurement [6]	4.85	46.6
This Method	4.862	40.63

necessary to obtain good accuracy in determining resonant frequencies, although this case is not considered.

The basis set is slightly modified if the rectangular DR is sitting on a ground plane. For this geometry, we have one PEC wall and five PMC walls. Therefore, we may start at one-quarter and increase with half-integers in the indexes because the lowest mode in this direction will be like a quarter-wave and the following higher order modes in this direction will increase in multiple half-wavenumbers, i.e., $p = 1/4, 3/4, 5/4, \cdots$.

IV. NUMERICAL RESULTS AND DISCUSSION

A. DR's in Free Space

Convergence tests are performed to validate the presented formulation. Since many results for cylindrical resonators immersed in free space are available in the literature, we study the $\mathrm{TE}_{01\delta}$ mode of a cylindrical DR by applying PMC basis functions (A3). The result of a convergence test for the complex frequency as a function of the number (N) of basis functions and mode types are shown in Table I. For a DR with $\varepsilon_d = 38\varepsilon_0$, $R = 5.25$ (mm), $D = 4.6$ (mm), where $R =$ radius and $D =$ height, we can see the solution has approximately converged at $N = 5$. If we look at the null space of (7), the (0, 1, 0) mode is dominant. The azimuthal indexes n are zero and the radial indexes m can be any integers, and only even integers of the z-direction indexes have contributions. The complex resonant frequency is compared to the results from other methods, and is shown in Table II. The real part shows good agreement with the other methods. The Q-factor shows greater

TABLE III
CONVERGENCE TEST OF A RECTANGULAR DR IN FREE SPACE, PMC MODES, $\varepsilon_d = 37.84\varepsilon_0$, $a = b = 8.77$ (mm), AND $d = 3.51$ (mm)

N	(m,n,p)	f_{real} (GHz)	f_{imag} (GHz)
1	(1,1,0)	5.6851	0.08212
2	(1,1,2)	5.6654	0.07988
3	(1,3,0)		
4	(3,1,0)	5.6591	0.07723
5	(1,3,2)		
6	(3,1,2)	5.6587	0.07716
7	(1,5,0)		
8	(5,1,0)	5.6578	0.07680
9	(1,7,0)		
10	(7,1,0)	5.6574	0.07671
11	(1,9,0)		
12	(9,1,0)	5.6573	0.07668

TABLE IV
RESONANCE FREQUENCY AND Q-FACTOR USING PMC MODES IN THE IE
FORMULATION COMPARED TO OTHER RESULTS FOR A RECTANGULAR DR IN
FREE SPACE WITH $\varepsilon_d = 37.84\varepsilon_0$, $a = b = 8.77$ (mm), AND $d = 3.51$ (mm)

	Frequency(GHz)	Q-factor
Measurement [10]	5.684	31.5
PMC basis functions expansion	5.6578	36.83
Full 3-D expansion	5.6493	36.88
Pulse basis expansion [22]	5.65002	37.09

variation among methods, although the method presented here agrees with the null field and one of the FDTD methods. Some variability of the Q-factor is to be expected, especially for open structures, due to the sensitivity of the computation. Also, the measurement of the Q-factor is difficult, with different measurement techniques often leading to different value [21]. As such, the Q-factor is in general agreement with other methods. The next convergence test concerns a rectangular DR by again only applying PMC basis functions (A2). The results for the $TE^z_{11\delta}$ mode of a rectangular DR with $\varepsilon_d = 37.84\varepsilon_0$ and dimensions $a = b = 8.77$ (mm), $d = 3.51$ (mm) are shown in Table III. The solution has approximately converged at $N = 8$. The (1, 1, 0) mode is dominant as observed by the null space of (7). Only the modes with odd indexes in the x- and y-direction and even indices in the z-direction contribute to the solution. In Table IV, we show measurement results and the results of using the full 3-D expansion set (A1) and using a MoM solution based on a subdomain pulse basis expansion [22]. In the full 3-D expansion, we use 136 terms in the E_x and 136 terms in the E_y expansion, although only 34 terms appear to contribute in the null space; ten PMC modes (20 terms), two PEC terms, and 12 other terms. Good agreement is seen between the full 3-D expansion and the eight modes (16 terms) PMC solution.

In Table V, we consider a hybrid mode (HE_{111}) of a rectangular DR in free space with $a = b = 3$ cm, $d = 1.5$ cm, for two different permittivity values, where the resonant frequencies are compared with results from [22]. The designation HE_{111} is de-

TABLE V
COMPARISON OF COMPLEX RESONANT FREQUENCIES OF THE HE_{111} MODE OF
AN ISOLATED RECTANGULAR DR IN FREE SPACE, COMPUTED WITH $N = 8$
PMC MODES, WITH $a = b = 3$ cm, $d = 1.5$ cm

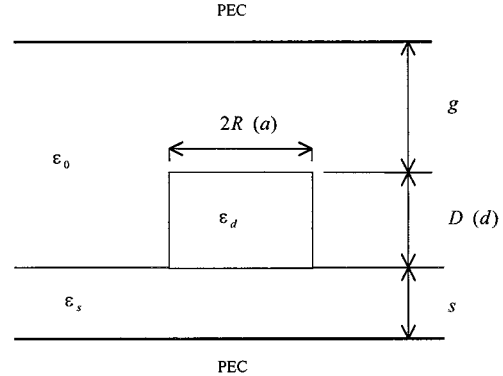|	f_{real} (GHz)	$f_{imag.}$ (GHz)
PMC ($\varepsilon_d = 15\varepsilon_0$)	3.69311	0.04478
Pulse Basis Function [22]	3.68987	0.04616
PMC ($\varepsilon_d = 20\varepsilon_0$)	3.23375	0.02211
Pulse Basis Function [22]	3.23326	0.02289

Fig. 3. Geometry of a cylindrical DR in a MIC environment.

termined by examination of the null space of (7). Good agreement is found among the two methods, with convergence properties of this hybrid mode being similar to those of the TE mode.

B. DR's in MIC Environments

When a DR is placed on a microstrip substrate, as depicted in Fig. 3, the background structure becomes inhomogeneous. In this case, we use an appropriate Green's function to account for the inhomogenity. For the shielded MIC cases, we show the comparison of our results using only PMC modes and results from the literature in Table VI(a)and (b) for a cylindrical resonator; agreement between all methods is good. Our results deviate more from the other results when the permittivity of the substrate is high. This is due to the fact that the permittivity ratio (inside to outside) of the DR at the interface becomes lower and further from a PMC boundary.

In Table VII(a)and (b), we present results for a rectangular DR in a shielded MIC environment, comparing the results using a PMC basis to those using the full solution (A1). Agreement is seen to be good between the two solutions, implying that the efficient PMC expansion is adequate. It is interesting to note that when the top and bottom conducting plates are close to the resonator, as in cases 1 and 2 in Table VII, in the full 3-D solution (A1) the terms corresponding to the top and bottom of the resonator obeying PEC conditions and the four sides obeying PMC conditions are dominant in the null space (the second term in (A1) for K^x and the 3rd term in (A1) for K^y). When the resonator is sufficiently separated from the top and bottom plates, the terms in (A1) corresponding to PMC conditions on all sides are dominant, as expected. Since (8) is stationary, the computed resonance frequency is accurate using just the PMC modes, even for cases 1 and 2.

Another MIC geometry is an open (unshielded) structure. Fig. 4 shows the results using this method and the results from

TABLE VI
(a) COMPARISON OF THE RESONANT FREQUENCY (IN GIGAHERTZ) FOR THE $TE_{01\delta}$ MODE OF A CYLINDRIVAL DR IN A SHIELDED MIC ENVIRONMENT. (b)
COMPARISON OF THE DIELECTRIC QUALITY FACTOR FOR THE $TE_{01\delta}$ MODE OF A CYLINDRICAL DR IN A SHIELDED MIC ENVIRONMENT

Case	ε_d	ε_s	R(mm)	D(mm)	s(mm)	g(mm)	Mode Matching	FD-SIC [25]	This Method
1	34.19	9.6	7.49	7.48	0.7	0.72	4.348 [23]	4.351	4.3645
2	34.21	9.6	6.995	6.95	0.7	1.25	4.523 [23]	4.524	4.5422
3	34.02	9.6	5.995	5.98	0.7	2.215	5.050 [23]	5.052	5.0869
4	36.13	9.6	3.015	4.21	0.7	10.10	8.220 [23]	8.223	8.2670
5	36.2	1.0	2.03	5.15	2.93	2.93	10.50 [24]	10.50	10.521
6	36.2	1.0	4.00	2.14	4.43	4.43	7.76 [24]	7.751	7.760

(a)

Case	$\tan\delta_{DR} \times 10^4$	FD-SIC [25]	This Method
1	3.02	3333	3337
2	3.19	3159	3163
3	3.47	2915	2918
4	4.22	2454	2437

(b)

TABLE VII
(a) COMPARISON OF THE RESONANT FREQUENCY (IN GIGAHERTZ) FOR THE $TE_{11\delta}^z$ MODE OF A RECTANGULAR DR IN A SHIELDED MIC ENVIRONMENT. (b)
COMPARISON OF THE DIELECTRIC Q FACTOR FOR THE $TE_{11\delta}^z$ MODE OF A RECTANGULAR DR IN A SHIELDED MIC ENVIRONMENT

Case	ε_d	ε_s	$a = b$ (mm)	d (mm)	s(mm)	g(mm)	PMC	Full 3-D	Difference (%)
1	34.19	9.6	14.98	7.48	0.7	0.72	4.2244	4.2096	0.35
2	34.21	9.6	13.99	6.95	0.7	1.25	4.3868	4.3746	0.28
3	34.02	9.6	11.99	5.98	0.7	2.215	4.8936	4.8834	0.21
4	36.13	9.6	6.03	4.21	0.7	10.10	7.8455	7.8330	0.16
5	36.2	1.0	4.06	5.15	2.93	2.93	9.8580	9.8426	0.16
6	36.2	1.0	8.00	2.14	4.43	4.43	7.4023	7.3978	0.06

(a)

Case	$\tan\delta_{DR} \times 10^4$	PMC	Full 3-D	Difference (%)
1	3.02	3341	3340	0.03
2	3.19	3167	3166	0.03
3	3.47	2923	2921	0.07
4	4.22	2453	2448	0.21

(b)

the effective dielectric constant (EDC) method and experiment [26]. Also in Fig. 4, the results for a rectangular DR with the same permittivity, volume, and height as the cylindrical DR are shown.

C. Open Coupled DR's

The complex resonant frequencies of coupled resonators are now considered. In general, the coupled-resonator structure possessing symmetry as shown in Fig. 5 can be divided into even modes and odd modes [27]. The even mode with a electric wall in the center plane of two DR's has a higher real resonant frequency and a larger Q-factor. The odd mode with magnetic wall in the center plane of the two DR's has a lower real resonant frequency and a smaller Q-factor. The resonant frequencies and Q-factors versus the separation g of two DR's are shown in Fig. 6. In the same plot, the comparison to the results using the null–field method [28] are also given. For the first time, the results of coupled rectangular resonators are also plotted in Fig. 6. The comparison shows that the real resonant frequency of the

even mode deviates from the null–field solution when the two resonators are extremely close. The reason is that the closest end faces between the two disks for the even mode should become like a perfect electric wall rather than a perfect magnetic wall. Therefore, the pure PMC basis function may not be adequate for this special situation. It is noted that computing resonant frequencies of a single DR above a ground plate can generate the results for the even modes of coupled DR's using the same basis functions to expand the electric field in one DR region.

V. CONCLUSION

The EFIE in conjunction with an entire-domain Galerkin's MoM is an efficient method for the analysis of separable-coordinate geometry DR's immersed in inhomogeneous media. It is shown that the PMC-mode basis functions are usually sufficient for practical DR's, and lead to solutions exhibiting strong numerical convergence. The method is particularly useful for rectangular resonators or, generally, nonbody-of-revolution geometries. The numerical results show good agreement with the
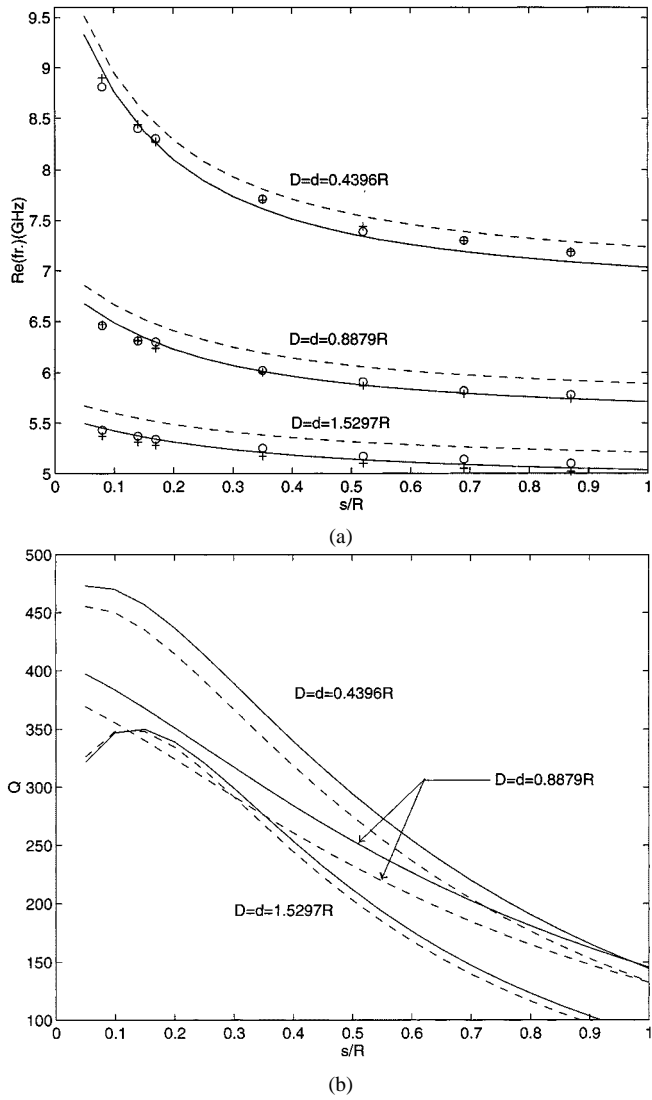
(a)

(b)

Fig. 4. Resonant frequencies and Q-factors of the $\text{TE}_{01\delta}$ mode of a cylindrical DR with $\varepsilon_d = 37.1\varepsilon_0$, $R = 4.55$ (mm) on a grounded substrate with $\varepsilon_s = 2.22\varepsilon_0$, and the $\text{TE}_{11\delta}^z$ mode of a rectangular DR with $\varepsilon_d = 37.1\varepsilon_0$, $a = b = 8.065$ (mm) on a grounded substrate with $\varepsilon_s = 2.22\varepsilon_0$. Solid lines: Cylindrical DR. Dashed lines: Rectangular DR. O:Experimental results. +: EDC results from [26] for a cylindrical DR.

literature for resonators immersed either in free space or in planarly layered environments.

APPENDIX

3-D basis functions for a rectangular cavity $[a \times b \times d]$ are shown below.

The full set of product terms are as follows:

$$\vec{K}_{(m,n,p)}(\vec{r})$$
$$= \hat{x}K_{(m,n,p)}^x(\vec{r}) + \hat{y}K_{(m,n,p)}^y(\vec{r}) + \hat{z}K_{(m,n,p)}^z(\vec{r})$$
$$K_{(m,n,p)}^\alpha(\vec{r})$$
$$= a_{mnp}^{\alpha 1} \sin \frac{m\pi}{a}\left(x + \frac{a}{2}\right) \sin \frac{n\pi}{b}\left(y + \frac{b}{2}\right) \sin \frac{p\pi}{d} z$$
$$+ a_{mnp}^{\alpha 2} \sin \frac{m\pi}{a}\left(x + \frac{a}{2}\right) \cos \frac{n\pi}{b}\left(y + \frac{b}{2}\right) \sin \frac{p\pi}{d} z$$
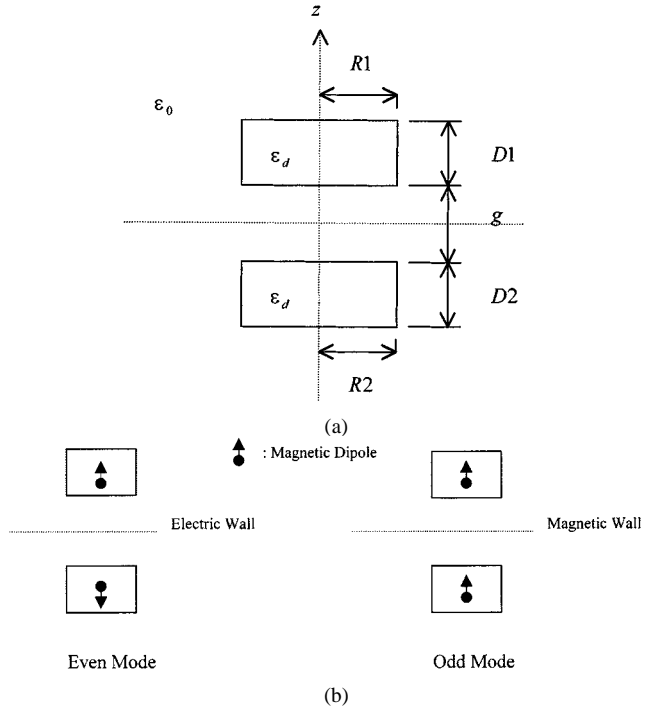

(a)

Even Mode   Odd Mode

(b)

Fig. 5. Geometry of coupled DR's and definitions of even and odd modes.

$$+ a_{mnp}^{\alpha 3} \cos \frac{m\pi}{a}\left(x + \frac{a}{2}\right) \sin \frac{n\pi}{b}\left((y + \frac{b}{2}\right) \sin \frac{p\pi}{d} z$$
$$+ a_{mnp}^{\alpha 4} \cos \frac{m\pi}{a}\left(x + \frac{a}{2}\right) \cos \frac{n\pi}{b}\left(y + \frac{b}{2}\right) \sin \frac{p\pi}{d} z$$
$$+ a_{mnp}^{\alpha 5} \sin \frac{m\pi}{a}\left(x + \frac{a}{2}\right) \sin \frac{n\pi}{b}\left(y + \frac{b}{2}\right) \cos \frac{p\pi}{d} z$$
$$+ a_{mnp}^{\alpha 6} \sin \frac{m\pi}{a}\left(x + \frac{a}{2}\right) \cos \frac{n\pi}{b}\left(y + \frac{b}{2}\right) \cos \frac{p\pi}{d} z$$
$$+ a_{mnp}^{\alpha 7} \cos \frac{m\pi}{a}\left(x + \frac{a}{2}\right) \sin \frac{n\pi}{b}\left(y + \frac{b}{2}\right) \cos \frac{p\pi}{d} z$$
$$+ a_{mnp}^{\alpha 8} \cos \frac{m\pi}{a}\left(x + \frac{a}{2}\right) \cos \frac{n\pi}{b}\left(y + \frac{b}{2}\right) \cos \frac{p\pi}{d} z$$

(A1)

where $\alpha = x, y, z$.

PMC cavity terms:

$$\vec{K}_{(m,n,p)}(\vec{r}) = \hat{x}K_{(m,n,p)}^x(\vec{r}) + \hat{y}K_{(m,n,p)}^y(\vec{r}) + \hat{z}K_{(m,n,p)}^z(\vec{r}). \quad (A2)$$

TE_{mnp} modes

$$K_{(m,n,p)}^x = \frac{-j\omega\mu_0(n\pi/b)}{\left(\frac{m\pi}{a}\right)^2 + \left(\frac{n\pi}{b}\right)^2}$$
$$\cdot \left[\sin \frac{m\pi}{a}\left(x + \frac{a}{2}\right) \cos \frac{n\pi}{b}\left(y + \frac{b}{2}\right) \cos \frac{p\pi}{d} z\right]$$

$$K_{(m,n,p)}^y = \frac{j\omega\mu_0(m\pi/a)}{\left(\frac{m\pi}{a}\right)^2 + \left(\frac{n\pi}{b}\right)^2}$$
$$\cdot \left[\cos \frac{m\pi}{a}\left(x + \frac{a}{2}\right) \sin \frac{n\pi}{b}\left(y + \frac{b}{2}\right) \cos \frac{p\pi}{d} z\right].$$

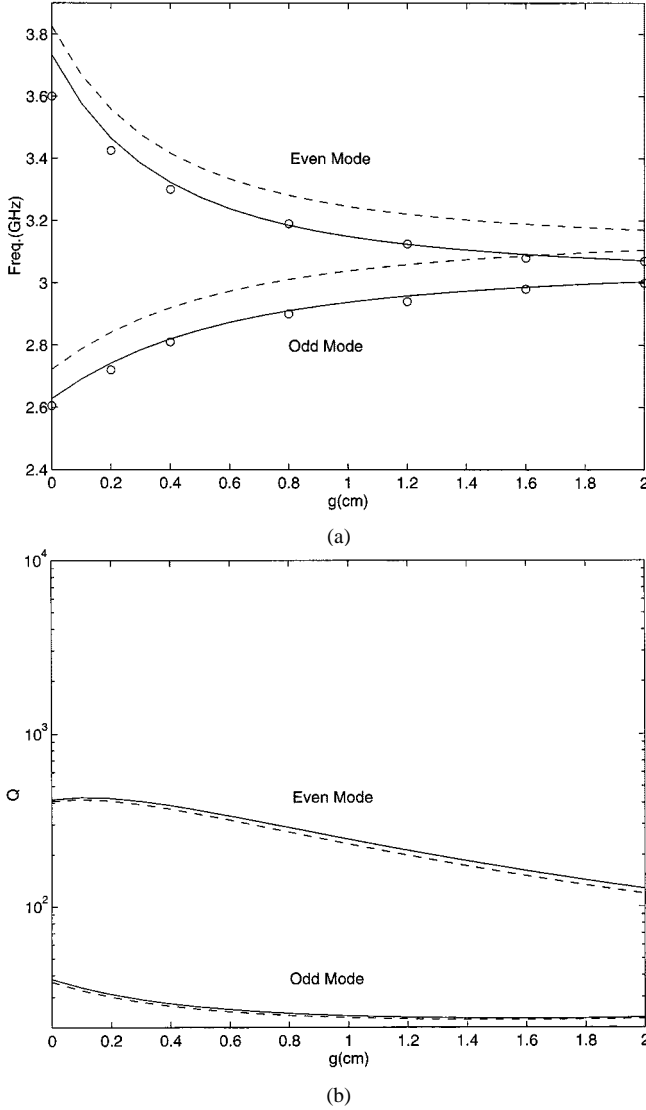Fig. 6. Resonant frequencies and Q-factors for the $\text{TE}_{01\delta}$ mode of open coupled cylindrical DR's and the $\text{TE}^z_{11\delta}$ mode of open coupled rectangular DR's Cylindrical DR's: $R1 = R2 = 0.8636$ (cm), $D1 = D2 = 0.762$ (cm), $\varepsilon_d = 35.74\varepsilon_0$. Rectangular DR's: $a1 = a2 = b1 = b2 = 2.165$ (cm), $d1 = d2 = 0.762$ (cm), $\varepsilon_d = 35.74\varepsilon_0$. Solid lines: cylindrical DR's. Dashed lines: rectangular DR's. o: results from [28] for cylindrical DR's.

TM_{mnp} modes

$$K^x_{(m,n,p)} = \frac{(m\pi/a)(p\pi/d)}{\left(\frac{m\pi}{a}\right)^2 + \left(\frac{n\pi}{b}\right)^2}$$
$$\cdot \left[\sin \frac{m\pi}{a} \left(x + \frac{a}{2}\right) \cos \frac{n\pi}{b} \left(y + \frac{b}{2}\right) \right.$$
$$\left. \cdot \cos \frac{p\pi}{d} z \right]$$

$$K^y_{(m,n,p)} = \frac{(n\pi/b)(p\pi/d)}{\left(\frac{m\pi}{a}\right)^2 + \left(\frac{n\pi}{b}\right)^2}$$
$$\cdot \left[\cos \frac{m\pi}{a} \left(x + \frac{a}{2}\right) \sin \frac{n\pi}{b} \left(y + \frac{b}{2}\right) \right.$$
$$\left. \cdot \cos \frac{p\pi}{d} z \right]$$

TABLE A1
BOUNDARY CONDITIONS ENFORCED BY TERMS OF (A1) AT VARIOUS SIDES OF RECTANGULAR RESONATOR FOR CURRENT COMPONENT $K^x_{(m,n,p)} (K^y_{(m,n,p)})$

Term Number	Top/Bottom BC	x-Sides BC	y-Sides BC
1	PEC (PEC)	PMC (PEC)	PEC (PMC)
2	PEC (PEC)	PMC (PEC)	PMC (PMC)
3	PEC (PEC)	PEC (PMC)	PEC (PMC)
4	PEC (PEC)	PEC (PMC)	PMC (PEC)
5	PMC (PMC)	PMC (PEC)	PEC (PMC)
6	PMC (PMC)	PMC (PEC)	PMC (PMC)
7	PMC (PMC)	PEC (PMC)	PEC (PMC)
8	PMC (PMC)	PEC (PMC)	PMC (PEC)

$$K^z_{(m,n,p)} = -\cos \frac{m\pi}{a} \left(x + \frac{a}{2}\right) \cos \frac{n\pi}{b} \left(y + \frac{b}{2}\right)$$
$$\cdot \sin \frac{p\pi}{d} z.$$

Cylindrical cavity ($R = \text{radius}$ and $D = \text{height}$) PMC modes

$$\vec{K}_{(n,m,p)}(\vec{r}) = \hat{\rho} K^\rho_{(n,m,p)}(\vec{r}) + \hat{\theta} K^\theta_{(n,m,p)}(\vec{r}) + \hat{z} K^z_{(n,n,p)}(\vec{r}) \tag{A3}$$

TE_{0mp} modes

$$K^\rho_{(0,m,p)} = 0$$
$$K^\theta_{(0,m,p)} = \frac{j\omega\mu_0}{\kappa_c} J'_0(\kappa_c\rho) \cos\left(\frac{p\pi}{D} z\right)$$
$$K^z_{(0,m,p)} = 0$$
$$\kappa_c = p_{0m}/R$$

where $J_n(x)$ is the Bessel function of the first kind and p_{nm} is the mth root of $J_n(x) = 0$; i.e., $J_n(p_{nm}) = 0$.

TM_{0mp} modes

$$K^\rho_{(0,m,p)} = \frac{(p\pi/D)}{\kappa_c} J'_0(\kappa_c\rho) \cos\left(\frac{p\pi}{D} z\right)$$
$$K^\theta_{(0,m,p)} = 0$$
$$K^z_{(0,m,p)} = - J_0(\kappa_c\rho) \sin\left(\frac{p\pi}{D} z\right)$$
$$\kappa_c = p'_{0m}/R$$

where p'_{nm} is the mth root of $J'_n(x) = 0$; i.e., $J'_n(p'_{nm}) = 0$.

REFERENCES

[1] R. Mongia and P. Bhartia, "Dielectric resonator antennas—A review and general design relations for resonant frequencies and bandwidth," *Int. J. Microwave Millimeter-Wave Eng.*, vol. 4, pp. 230–347, July 1994.
[2] A. Glisson, D. Kajfez, and J. James, "Evaluation of mode in dielectric resonators using a surface integral equation formulation," *IEEE Trans. Microwave Theory Tech.*, vol. MTT-31, pp. 1023–1029, Dec. 1983.
[3] J. Pereda, L. Vielva, A. Vegas, and A. Prieto, "Computation of resonant frequencies and quality factors of open dielectric resonators by a combination of finite-difference time domain (FDTD) and Prony's methods," *IEEE Microwave Guided Wave Lett.*, vol. 2, pp. 431–433, Nov. 1992.

[4] A. Navarro and M. J. Nunez, "FDTD method coupled with FFT: A generalization to open cylindrical devices," *IEEE Trans. Microwave Theory Tech.*, vol. 42, pp. 870–874, May 1994.

[5] W. Zheng, "Computation of complex resonance frequencies of isolated composite objects," *IEEE Trans. Microwave Theory Tech.*, vol. 37, pp. 953–961, June 1989.

[6] R. Mongia, C. Larose, S. Mishra, and P. Bhartia, "Accurate measurement of Q-factors of isolated dielectric resonators," *IEEE Trans. Microwave Theory Tech.*, vol. 42, pp. 1463–1466, Aug 1994.

[7] R. E Collin, *Field Theory of Guided Waves*, New York:: IEEE Press, 1991.

[8] S. M. Shum and K. M. Luk, "Analysis of aperture coupled rectangular dielectric resonator antenna," *Electron. Lett.*, vol. 30, no. 21, pp. 1726–1727, Oct. 1994.

[9] R. W. Lyon and J. Helszajn, "Finite element analysis of planar circulators using arbitrarily shaped resonators," *IEEE Trans. Microwave Theory Tech.*, vol. MTT-30, pp. 1964–1974, Nov. 1982.

[10] R. Mongia and A. Ittiiboon, "Theoretical and experimental investigation of rectangular dielectric resonator antennas," *IEEE Trans. Antenna Propagat.*, vol. 45, pp. 1348–1356, Sept. 1997.

[11] C. A. Balanis, *Advanced Engineering Electromagnetics*, New York: Wiley, 1989.

[12] V. H. Rumsey, "The reaction concept in electromagnetic theory," *Phys. Rev.*, vol. 94, pp. 1483–1491, June 1954.

[13] E. W. Blumbergs, "Integral equation formulation for natural modes of a circular patch antenna in layered environment," Ph.D. dissertation, Dept. Elect. Eng., Michigan State Univ., Ann Arbor, MI, 1989.

[14] S.-L. Lin, "Propagation characteristics of anisotropic dielectric waveguides in the bound and leaky regimes," Ph.D. dissertation, Dept. Elect. Eng. Comput. Sci., Univ. Wisconsin at Milwaukee, Milwaukee, WI, 1995.

[15] W. C. Chew, *Waves and Fields in Inhomogeneous Media*, New York: Van Nostrand, 1990, pp. 118–120.

[16] E. H. Newman and D. Forrai, "Scattering from a microstrip patch," *IEEE Trans. Antenna Propagat.*, vol. AP-35, pp. 245–251, Mar. 1987.

[17] W. H. Press, S. A. Teukolsky, W. T. Vetterling, and B. P. Flannery, *Numerical Recipes*.   Cambridge, U.K.: Cambridge Univ. Press, 1992, p. 134.

[18] D. G. Dudley, "Comments on variational nature of Galerkin and non-Galerkin moment method solutions," *IEEE Trans. Antenna Propagat.*, vol. 45, pp. 1062–1063, June 1997.

[19] A. F. Peterson, D. R. Wilton, and R. E. Jorgenson, "Variational nature of Galerkin and non-Galerkin moment method solutions," *IEEE Trans. Antenna Propagat.*, vol. 44, pp. 500–503, Apr. 1996.

[20] I. V. Lindell, "Variational methods for nonstandard eigenvalue problems in waveguide and resonator analysis," *IEEE Trans. Microwave Theory Tech.*, vol. MTT-30, pp. 1194–1204, Aug. 1982.

[21] A. W. Glisson, "Integral equation techniques," in *Dielectric Resonators*, D. Kajfez and P. Guillon, Eds.   Norwood, MA: Artech House, 1986, ch. 6.

[22] K. Walters, private communication, June 1998.

[23] S. Maj and J. W. Modelski, "Application of a dielectric resonator on microstrip line for a measurement of complex permittivity," in *IEEE MTT-S Int. Microwave Symp. Dig.*, 1984, pp. 525–527.

[24] M. Jaworski and M. W Pospieszalski, "An accurate solution of the cylindrical dielectric resonator problem," *IEEE Trans. Microwave Theory Tech.*, vol. MTT-27, pp. 639–643, July 1979.

[25] J.-M. Guan and C.-C. Su, "Precise computations of resonant frequencies and quality factors for dielectric resonators in MIC's with tuning elements," *IEEE Trans. Microwave Theory Tech.*, vol. 45, pp. 439–442, Mar. 1997.

[26] R. K. Mongia, "Resonant frequency of cylindrical dielectric resonator placed on MIC environment," *IEEE Trans. Microwave Theory Tech.*, vol. 38, pp. 802–804, June 1990.

[27] J. Van Bladle, "Weakly coupled dielectric resonators," *IEEE Trans. Microwave Theory Tech.*, vol. MTT-30, pp. 1907–1914, Nov. 1982.

[28] W. Zhang, "Direct and inverse resonance problems for shielded composite objects treated by means of the null-field method," *IEEE Trans. Microwave Theory Tech.*, vol. 37, pp. 1732–1739, Nov. 1989.

Shu-Li Lin was born in Hsinchu, Taiwan, R.O.C., in 1962. He received the B.S. degree in physics from the Tunghai University, Taiwan, R.O.C., in 1985, the M.S. degree in engineering from the University of Wisconsin at Milwaukee, in 1995, and is currently working toward the Ph.D. degree at the University of Wisconsin at Milwaukee.

George W. Hanson (S'85–M'91–SM'98), for photograph and biography, see this issue, p. 75.